

## **Kinetic and Sorption Modelling of Photocatalytic Removal of Pb(II) In Paint Effluent Using TiO<sub>2</sub> Under Solar Irradiation**

*Osarumwense, J.O.<sup>1</sup> and Ejoboka, O.L<sup>2</sup>*

<sup>1,2</sup>Department of Science Laboratory Technology, Faculty of Life Sciences,  
University of Benin, Benin City.

### *Abstract*

---

*The kinetics and sorption modeling of photocatalytic removal of lead ion (Pb<sup>2+</sup>) in paint effluent using titanium dioxide (TiO<sub>2</sub>) was studied. The process was carried out in a batch system at different contact time and catalyst dosage under solar irradiation; and the residual metal ion in the solution was determined using atomic absorption spectrophotometer (AAS). The results showed that about 96% removal efficiency was achieved at optimum catalyst dosage of 1g/L, and the process attained equilibrium at 140 minutes. Pseudo-first order model with a rate constant of 0.0194min<sup>-1</sup> showed sufficient description of the kinetics of the process; and intraparticle diffusion model revealed that the uptake of Pb<sup>2+</sup> was more of the film diffusion than the intraparticle diffusion. Langmuir isotherm with a regression value, R<sup>2</sup>(0.931) and adsorption capacity (1.56L/mg) best described the sorption of Pb<sup>2+</sup> onto TiO<sub>2</sub>. Meanwhile, the heat of sorption (+3.2015 KJ/mol) obtained from Temkin isotherm indicates that the process was exothermic.*

---

**Keywords:** Adsorption capacity, lead, exothermic, film diffusion, solar irradiation.

### **1.0 Introduction**

Industrial effluent is a complex mixture of several classes of pollutants including synthetic chemicals of various description, hydrocarbons and heavy metals [1]. Paint and textile industries release effluents that can be in the form of solid, liquid or gaseous organic or inorganic substances. In the three forms of pollutants, the liquid effluent is the most significant and abundant [2]. Most industries discharge their untreated effluents through drains or canals into the nearest water body such as streams [3], while some others release their effluents into vegetation leading to a high bioaccumulation in the plants or soil [4]. Most industrial effluents contain high concentration of potentially mutagenic heavy metals, and it has been reported that heavy metals are among the most toxic and environmentally dangerous pollutants [5]. Quite a number of toxic heavy metals such as Lead (Pb), Chromium (Cr), Cadmium (Cd), Manganese (Mn), Copper (Cu), Zinc (Zn) etc. are present in paint effluent [6, 4]. Lead is a toxic substance, however some of its compounds are used as colour pigments and drying agent to improve luster in house-hood paints. The impact of lead in industrial effluents on aquatic and terrestrial ecosystems has drawn a lot of attention worldwide because of its overwhelming environmental significance [7]. Conventional methods for the removal of metal ion include adsorption, ion exchange, extraction etc. However, the use of adsorption techniques can only remove the metal ion from one site of the environment to another.

Heterogeneous photocatalysis facilitated by UV irradiated semiconductor oxide such as TiO<sub>2</sub> has been identified as a promising technique for the oxidation of organic and inorganic contaminants in liquid effluent [8]. The photocatalysis initiated by solar energy in the presence of a stable metal oxide as catalyst has been studied extensively [9]. On the absorption of photon energy ( $h\nu$ ) equal or greater than the band gap energy of the semiconductor (3.2 eV for anatase), an electron ( $e^-$ ) is excited from the valence band (VB) to the conduction band (CB) of the semiconductor. Simultaneously, an electron vacancy or a positively charged hole ( $h^+$ ) is created in the VB. The semiconductor then exhibits a void energy region in which no energy levels are available to promote the recombination of  $e^-$  and  $h^+$  produced by photo-activation in the solid [10]. A simplified mechanism for the photo-activation of a semiconductor catalyst is presented in Figure 1. Ultraviolet (UV) or near-ultraviolet photons ( $\lambda < 387$  nm) are typically required for this kind of reaction [11]. The valence band  $h^+$  is strongly oxidizing, and the conduction band  $e^-$  is strongly reducing. At the external surface, the excited electron and the hole can take part in

---

Corresponding author: Osarumwense, J.O., E-mail: judeosarumwense@uniben.edu, Tel.: +2348023297060

redox reactions with adsorbed species such as water. Generally, the  $h^+$  oxidizes water to hydroxyl radicals ( $OH^\cdot$ ) which subsequently initiate a chain of reactions leading to the oxidation of pollutant, or it can be combined with the electron from a donor species, depending on the mechanism of the photoreaction. Similarly, the electron can be donated to an electron acceptor such as an oxygen molecule leading to formation of superoxide radical ( $O_2^{\cdot-}$ ) or a metal ion with a redox potential more positive than the band gap of the photocatalyst. The hydroxyl radical ( $OH^\cdot$ ) was proposed to be the primary oxidant in the photocatalytic system [12]. Lead (II) ion is oxidized to its higher valence state which is practically insoluble in aqueous solution and is thus filtered off. The electron-transfer process is more efficient if the species are pre-adsorbed on the surface of the catalyst [10].

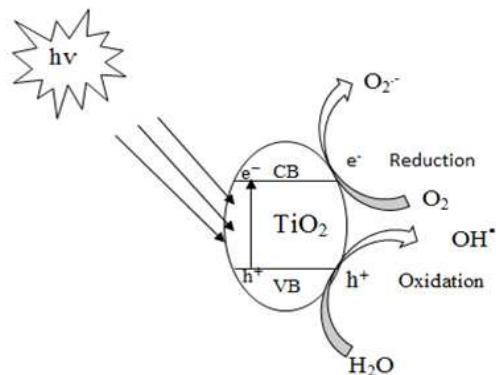
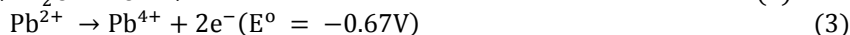
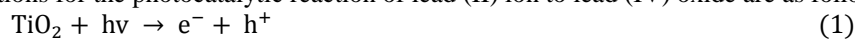


**Figure 1:** A simplified mechanism for the photo-catalytic removal of  $Pb^{2+}$  [13]

Simple chemical equations for the photocatalytic reaction of lead (II) ion to lead (IV) oxide are as follows;



As a result of the toxic nature of lead to organisms in the environment, it is necessary to carry out a thorough assessment of lead content in paint effluent, and then reduce the concentration to acceptable level before discharge into the environment. Therefore, this study was focused on the photocatalytic removal of  $Pb^{2+}$  in paint effluent using titanium dioxide as catalyst under the sun. Lead and Cadmium have been removed by photocatalytic process using  $TiO_2$  irradiated by artificial UV-lamp [14], while chromium (IV) has been removed by carbon modified (CM)-n- $TiO_2$  nanoparticles under solar irradiation [13].

## 2.0 Methodology

### 2.1 Materials

Paint effluent, reddish in colour, was collected from a small-scale paint producer in Benin City. The sample was stored in a clean plastic can and kept in a refrigerator at  $4^\circ C$ . The pH of the effluent was measured, and the effluent was used in all experiments without further dilution. Anatase form of  $TiO_2$ , a product of BDH chemical Ltd, England with an average particle size of 21 nm and surface area (BET) of  $50 \pm 15 m^2/g$  was used as catalyst.

### 2.2 Photocatalytic Studies

The photocatalytic removal of  $Pb^{2+}$  was conducted in a batch system. A certain volume (200ml) of paint effluent was measured into different conical flasks (500ml) containing 0.05g, 0.1g, 0.15g, 0.2g, 0.25g of  $TiO_2$ , and control (no catalyst). The flasks were placed on a flat orbital shaker (Optima OS-752 model) operated at a speed of 120 rpm for continuous shaking under the sun (temperature,  $32 \pm 2^\circ C$ ) for 3 hours. The experiment was repeated in the laboratory using air bath shaker (Model THZ-82) without sunlight; the conical flasks were wrapped with aluminium foil to prevent penetration of UV rays [15]. Samples were collected from each flask at predetermined time to evaluate the effect of irradiation time and catalyst dosage, the samples were filtered using fine crystalline filter paper (Whatman number 42). The filtered samples were analysed using AAS (Solar 969 model, Unicam series). The percentage removal efficiency of  $Pb^{2+}$  was obtained from the equation:

$$\% \text{ Removal} = \frac{C_i - C_f}{C_i} \times 100 \quad (5)$$

$C_i$  and  $C_f$  are the initial and final concentration of  $Pb^{2+}$  in solution.

### 2.3 Kinetic Model Equations

The experimental data were subjected to kinetic models such as pseudo-first order, pseudo second order and intra-particle diffusion models, to determine the kinetic parameters and rate-limiting step of the process.

**Pseudo-first order kinetic equation**

$$\frac{dq}{dt} = K_1(q_e - q_t) \tag{6}$$

Where,  $q_e$  and  $q_t$  are the amounts of  $Pb^{2+}$  removed at equilibrium and time  $t$ , respectively per unit mass of the catalyst (mg/g); and  $K_1$  is the pseudo first-order rate constant. After integration and applying boundary conditions  $t = 0$  to  $t = t$  and  $q_t = 0$  to  $q_t = q_t$  equation (6) becomes:

$$\log(q_e - q_t) = \log q_e - \frac{K_1}{2.303} t \tag{7}$$

The plot of  $\log(q_e - q_t)$  against  $t$  gives a linear relationship where  $K_1$  and  $q_e$  were determined from the slope and intercept of the plot, respectively [16, 17].

**Pseudo-second order kinetic equation**

The pseudo second-order adsorption kinetic rate equation is expressed as:

$$\frac{dq}{dt} = K_2(q_e - q_t)^2 \tag{8}$$

$K_2$  is the rate constant of pseudo second-order adsorption (g/mg.min). Linearizing equation (8) for the boundary conditions  $t = 0$  to  $t = t$  and  $q_t = 0$  to  $q_t = q_t$ , becomes:

$$\frac{1}{q_e - q_t} = \frac{1}{q_e} + K_2 t \tag{9}$$

Further rearrangement of equation (9) gives the following:

$$\frac{t}{q_t} = \frac{1}{K_2 q_e^2} + \frac{1}{q_e} t \tag{10}$$

and  $h = K_2 q_e^2$ , where  $h$  is the initial rate of sorption (mg/g)

The plot of  $t/q_t$  against  $t$  yield a straight line where  $K_2$  can be calculated [16, 17]

**Intra particle diffusion-controlled sorption**

To investigate the internal diffusion mechanism during photocatalytic process, the intra-particle diffusion equation has been used, considering that adsorption is usually controlled by an external film resistance and internal or intra-particle diffusion [18]. For adsorption onto spherical particles with constant diffusion coefficient, Crank [19] proposed the following equation:

$$q_t = K_{id} t^{0.5} \tag{11}$$

The coefficient  $k_{id}$  is determined from the linear plot of  $qt$  versus (time)<sup>0.5</sup>. Good linearization of data is normally observed for the initial phase of reaction in accordance with expected behavior if intra particle diffusion is rate limiting [20]. The intra particle diffusion plot of  $q_t$  versus  $t^{0.5}$  should be linear. If the plot is not completely linear, and do not pass through the origin, then the intra particle diffusion cannot be the only mechanism involved [21]. According to previous work [22], if the intra-particle diffusion plot does not pass through the origin, then equation (11) becomes:

$$q_t = K_{id} t^{0.5} + C_{id} \tag{12}$$

Where  $C_{id}$  is intra particle diffusion constant or intercept of the line (mg/g). It is directly proportional to the boundary layer. Apart from the linearity of the intra particle diffusion plot, the sorption mechanism assumes intra particle diffusion if the following are met:

- i. High coefficient of determination ( $R^2$ ) to ascertain applicability
- ii. Straight line which passes through the origin
- iii. Intercept  $C_{id} < 0$ .

Deviation from (ii) and (iii) above shows that the mode of transport is affected by more than one process [22].

**2.4 Adsorption Isotherms**

Adsorption isotherms relate the concentration of solute on the surface of the adsorbent to the concentration of the solute in the fluid with which the adsorbent is in contact. For single metal adsorption, Langmuir, Freundlich and Temkin isotherm models were used to establish the adsorption isotherms of photocatalytic removal of  $Pb^{2+}$ .

**Freundlich Isotherm**

Freundlich isotherm is commonly used to describe the adsorption characteristics for the heterogeneous surface [23]. The experimental data often fit to the empirical equation as shown:

$$q_e = K_f C_e^{1/n} \tag{13}$$

The constants associated with the Freundlich isotherm model are sorption capacity ( $K_f$ ) and sorption intensity ( $1/n$ ). These parameters provide an indication for the capacity of the adsorbent/adsorbate system and favourability of the isotherm, respectively.  $C_e$  is the equilibrium concentration of adsorbate (mg/L), and  $q_e$  is the amount of metal adsorbed per gram of the adsorbent at equilibrium (mg/g).

Linearizing equation (13), we have:

$$\log q_e = \log K_f + \frac{1}{n} \log C_e \quad (14)$$

The slope,  $1/n$  ranges from 0 and 1, it is also a measure of surface heterogeneity. The system become more heterogeneous as the value gets closer to zero [24]. If  $1/n$  is equal to 1, then the partition between the two phases are independent of the concentration. If value of  $1/n$  is below one, it indicates a normal adsorption. On the other hand,  $1/n$  above one indicates cooperative adsorption [25, 26].

### Langmuir isotherm

This isotherm describes quantitatively, the formation of a monolayer adsorbate on the outer surface of the adsorbent, and after that no further adsorption takes place. Thereby, the Langmuir model represents the equilibrium distribution of adsorbate between the solid and liquid phases [27]. The Langmuir isotherm is valid for monolayer adsorption onto a surface containing a finite number of identical sites. The model assumes uniform energies of adsorption onto the surface and no transmigration of adsorbate in the plane of the surface. Based upon these assumptions, Langmuir proposed the following equation:

$$q_e = \frac{Q_0 K_L C_e}{1 + K_L C_e} \quad (15)$$

Langmuir adsorption parameters were determined by transforming the Langmuir equation (15) into linear form

$$\frac{1}{q_e} = \frac{1}{Q_0} + \frac{1}{Q_0 K_L C_e} \quad (16)$$

Where;  $C_e$  is the equilibrium concentration of adsorbate (mg/L).

$q_e$  is the amount of metal adsorbed per gram by the adsorbent at equilibrium (mg/g).

$Q_0$  is maximum monolayer coverage capacity (mg/g).

$K_L$  is Langmuir isotherm constant (L/mg). The values of  $Q_0$  and  $K_L$  were computed from the slope and intercept of the Langmuir plot of  $1/q_e$  versus  $1/C_e$  [28].

The essential features of the Langmuir isotherm may be expressed in terms of equilibrium parameter  $R_L$ , which is a dimensionless constant, also referred to as separation factor [29].

$$R_L = \frac{1}{1 + (K_L C_0)} \quad (17)$$

where  $C_0$  is initial concentration.

The value of  $R_L$  indicates the shape of the isotherm to be linear ( $R_L=1$ ), unfavourable ( $R_L>1$ ), irreversible ( $R_L=0$ ) and favourable ( $0 < R_L < 1$ ) [30].

### Temkin isotherm model

Temkin model was used to test the adsorption potential of  $TiO_2$ . The model takes into account the effect of indirect adsorbent/adsorbate interaction on the adsorption process; and it is assumed that the heat of adsorption ( $\Delta H_{ads}$ ) of all molecules in the layer decreased linearly by increasing the coverage area [30]. The simplest form of Temkin isotherm is given as follows:

$$q_e = \frac{RT}{b_T} \ln(K_T C_e) \quad (18)$$

The linear form of equation (18) is given as follows:

$$q_e = \frac{RT}{b_T} \ln K_T + \frac{RT}{b_T} \ln C_e \quad (19)$$

where,  $R$  is gas constant (0.008314 KJ/mol.K),  $T$  is the absolute temperature (K),  $1/b_T$  is the Temkin constant related to the heat of sorption (KJ/mol) which indicates the adsorption potentials of the adsorbent, and  $K_T$  (L/g) is Temkin constant related to adsorption capacity.

## 3.0 Results and Discussion

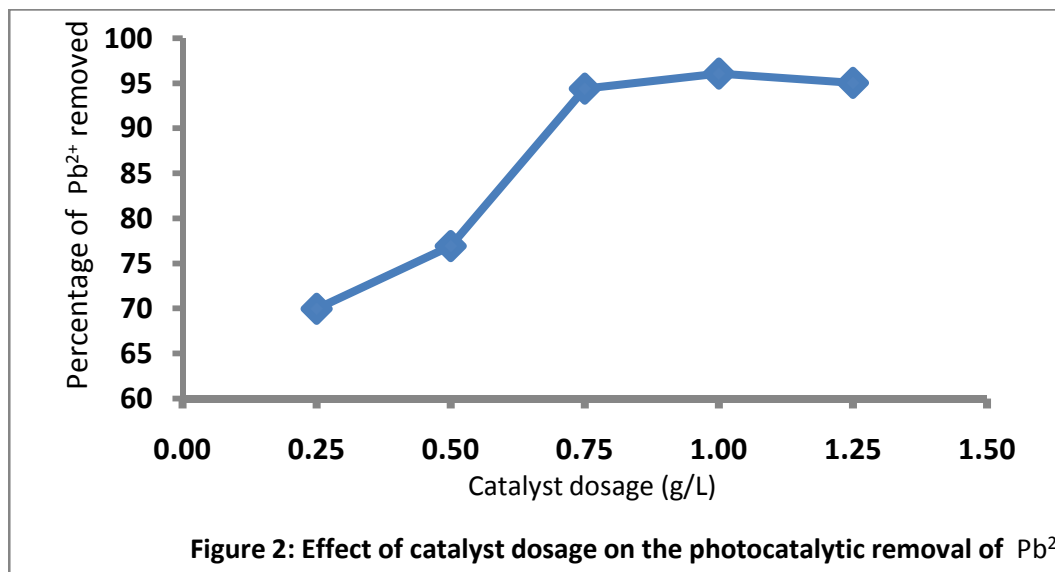
### 3.1 Assessment of Concentration of Lead in Paint Effluent

The pH and the initial concentration of  $Pb^{2+}$  were determined in the paint effluent. The effluent has a pH value of 6.7 and  $Pb^{2+}$  content of 3.796mg/L. This concentration of  $Pb^{2+}$  is outside the recommended acceptable discharge limit of  $< 1.0$ mg/L set by the Federal Environment Protection Agency of Nigeria [31]. This is an indication that the effluent was highly contaminated with  $Pb^{2+}$  and the disposal of such effluent without treatment will pose an adverse lead poisoning to both terrestrial and aquatic organisms in the environment.

### 3.2 Effect of Catalyst Dosage

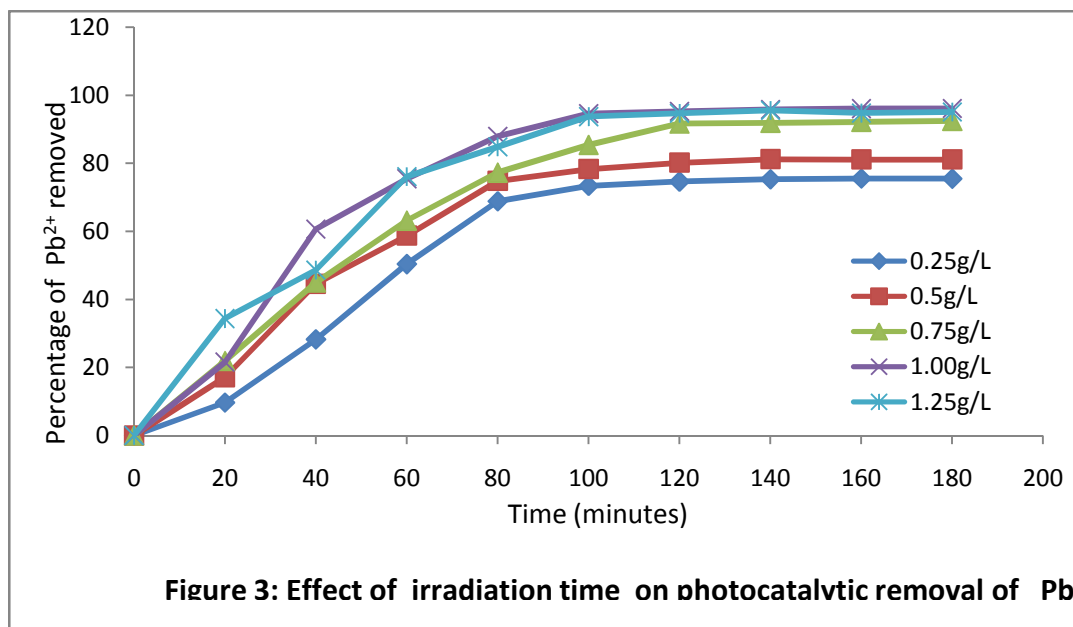
The effect of catalyst ( $TiO_2$ ) dosage on the photocatalytic removal of  $Pb^{2+}$  ion in paint effluent is shown in Figure 2. The catalyst ( $TiO_2$ ) dosage was varied from 0.25g/L to 1.25g/L. The result shows that the percentage removal of  $Pb^{2+}$  increased

with increasing catalyst dose up to an optimum point and then decreased. From the result, it was observed that the percentage removal increased from 70% to 96% as the catalyst concentration increases from 0.25g/L to 1.0g/L, and further increase of the catalyst concentration to 1.25g/L, the percentage removal decreased to 93%. Thus, 1.0g/L was the optimum catalyst concentration for the process. An optimum  $\text{TiO}_2$  dosage of 0.9g/L has been reported in literature for the removal of lead and cadmium with UV-lamp irradiated photocatalytic process [14]. The initial increase in percentage removal could be due to the increase in the number of active sites on the catalyst surface as a result of increased catalyst dosage. Increasing the dosage of catalyst, the number of free radical ( $\text{OH}^\bullet$ ) in solution were also increased consequently leading to enhanced photo-oxidation of the substrate in the effluent sample. The decreased in photo-oxidation as the catalyst concentration was increased beyond the optimum dosage could be attributed to the suspended particles of the catalyst which aggregate together and then reduced the amount of sunlight reaching the active sites of the catalyst and consequently, the rate of reaction decreases. This is in conformity with the report from literature [32].



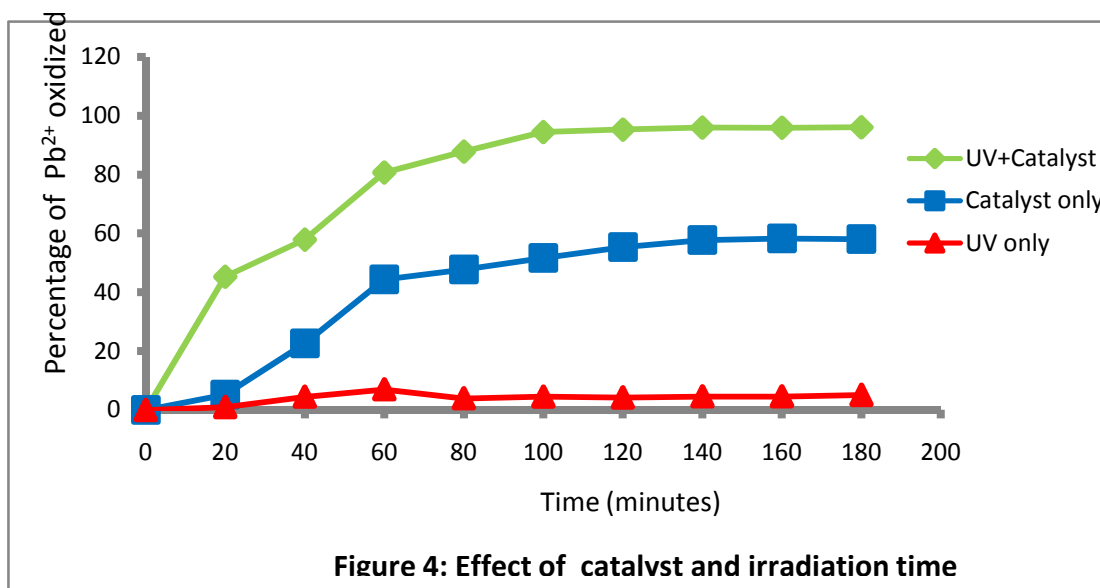
### 3.3 Effect of Irradiation Time

The effect of irradiation time on the photocatalytic removal of  $\text{Pb}^{2+}$  was investigated. Figure 3 clearly shows that sampling was carried out at an interval of 20 minutes for 3 hours. From the result, it was observed that the rate of  $\text{Pb}^{2+}$  removal was rapid in the first 60 minutes; it then became slower and almost constant at 140 minutes for all the catalyst concentration tested. At this point, the process was said to have reached equilibrium. The amount of  $\text{Pb}^{2+}$  removed at equilibrium was 75%, 81%, 92%, 96% and 95% for 0.25g/L, 0.5g/L, 0.75g/L, 1g/L and 1.25g/L respectively. Greater photon was absorbed by the catalyst at elongated irradiation time; however at equilibrium, the formation of lead oxide in the solution could impede the penetration of the photon energy thereby limiting the generation of hydroxyl radical. Secondly, the active sites of the catalyst would have been completely filled by the substrate and became saturated. This is in agreement with other reports in literature [33].



### 3.4 Effect of TiO<sub>2</sub> and UV Irradiation

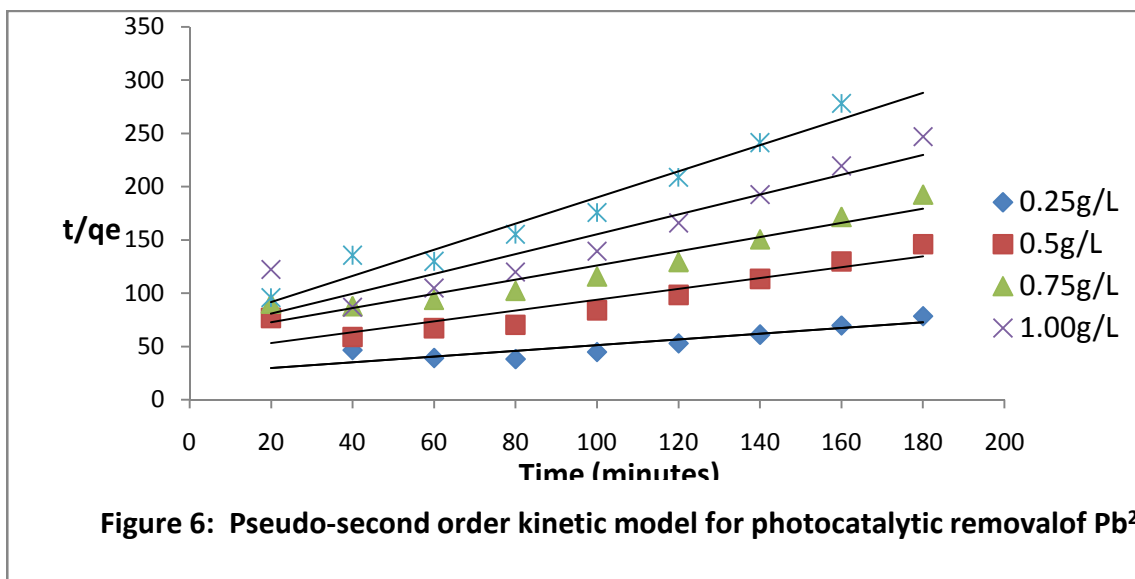
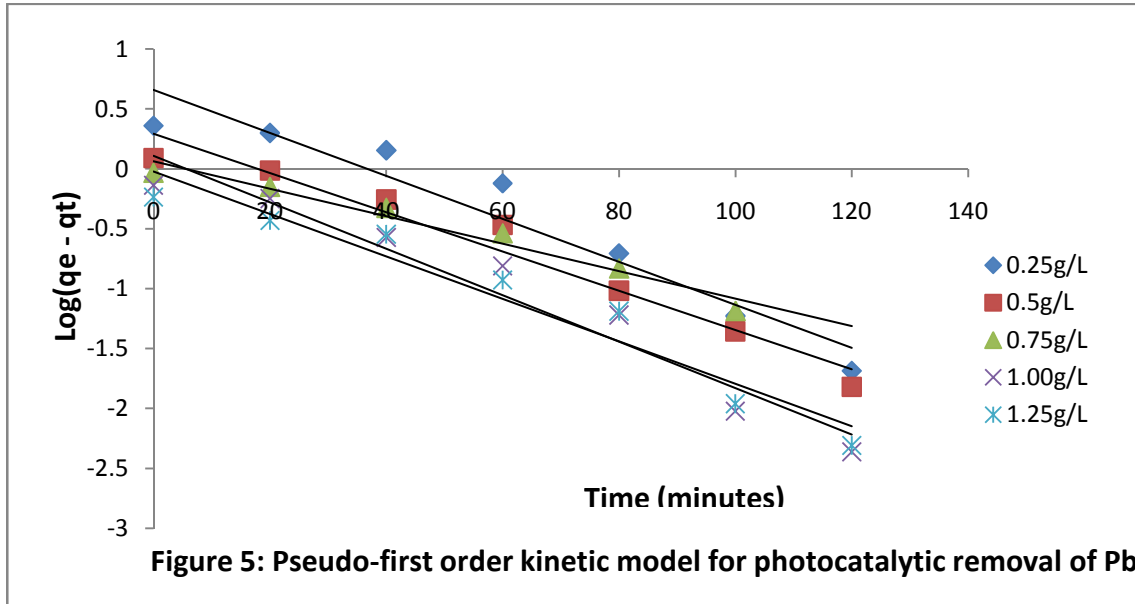
Control experiments were carried out to investigate the effects of sunlight and catalyst on the removal of Pb<sup>2+</sup>. As one set of experiment was carried out under the sun but without catalyst, another set was done with a concentration of 1.0mg/L TiO<sub>2</sub> in the laboratory without sunlight (dark experiment). The results of the control experiments in comparison with the one carried out in the presence of catalyst and sunlight are shown in Figure 4. From the result, it was deduced that sunlight and catalyst played prominent roles in the photocatalytic oxidation process, about 58 % removal of Pb<sup>2+</sup> was obtained at the dark (adsorption) experiment as against 96% with sunlight and catalyst, while no significant amount of Pb<sup>2+</sup> was removed with sunlight alone. This is in agreement with previous studies which reported that photocatalysis is initiated by photon energy (UV rays) in the presence of a stable metal oxide as catalyst for the degradation of organic and inorganic compounds[8, 9].



### 3.5 Kinetic Models

The linear plots of the kinetic models for the photocatalytic process are presented in Figures 5 and 6 for pseudo first-order and pseudo second-order models, respectively. The rate constants and other parameters were calculated and presented in Table 1. The coefficient of determination ( $R^2$ ) and the kinetic rate constants values revealed that the process fitted more to the pseudo first-order model than pseudo second-order model. For the optimum catalytic dosage of 1g/L, the rate constant ( $k_1$ ) of

0.0194min<sup>-1</sup> and R<sup>2</sup> of 0.9539 were obtained for pseudo-first order kinetic model while pseudo second-order models had rate constant (k<sub>2</sub>) of 1.4 x 10<sup>-2</sup>g/mg.min and R<sup>2</sup> of 0.8157. The R<sup>2</sup> represents the percent of the data closest to the line of best fit. R<sup>2</sup> for pseudo first order is 0.9539 which means that 95.39% of the total variation of data in y-axis can be explained by the linear relationship between y and x, that is, only 4.61% remains unexplained. In addition to the good linear model fit, the reaction rate constant suggested that photocatalytic removal of Pb<sup>2+</sup> followed pseudo first-order kinetics and that Pb<sup>2+</sup> were adsorbed onto the TiO<sub>2</sub> surface via chemical interaction. In another work, the pseudo first-order model was also found applicable when the photocatalytic properties of ZnO nanocrystal were investigated in the oxidation of insecticide diazinon [33].



The intra-particle diffusion often plays important role in adsorption process especially for porous adsorbent. It is a transport process involving movement of species from the bulk of the solution to the solid phase [34]. The kinetics data from this study were fitted into intra-particle diffusion model using equation (11). A linear plot of qt versus the square root of the time, gives the rate constant (slope of the plot). A non-regression coefficient plot gives a 3-phase plot viz. the initial (linear), second and third phases [22]. The linear stage corresponding to fast uptake of sorbate; and if the line in the initial stage does not pass through the origin, it denotes that uptake is dominated by film diffusion than it does for the intraparticle diffusion process. In the second stage, sorbate adsorption speeds up reflecting nonconsecutive diffusion of sorbate molecules into the micropores of the sorbent; and in the third phase, diffusion remains fairly constant when the pore volume is exhausted [35]. The linear

plot is shown in Figure 7. It comprises the initial phase of 60 minutes of the photocatalytic reaction. The intra-particle diffusion constants were calculated from the slopes of the linear plot and shown in Table 1. The regression lines in Figure 7 did not pass through the origin, and an intercept  $C_{id}$  was provided. This is an indication of the role of other rate-limiting steps of the process other than the intra particle diffusion. In addition, the  $K_{id}$  values are greater than 0, both intra-particle diffusion and external mass transfer (film diffusion) are considered as rate limiting steps. The value of  $C_{id}$  provides information related to the thickness of the boundary layer; and it is directly proportional to the boundary layer [20].

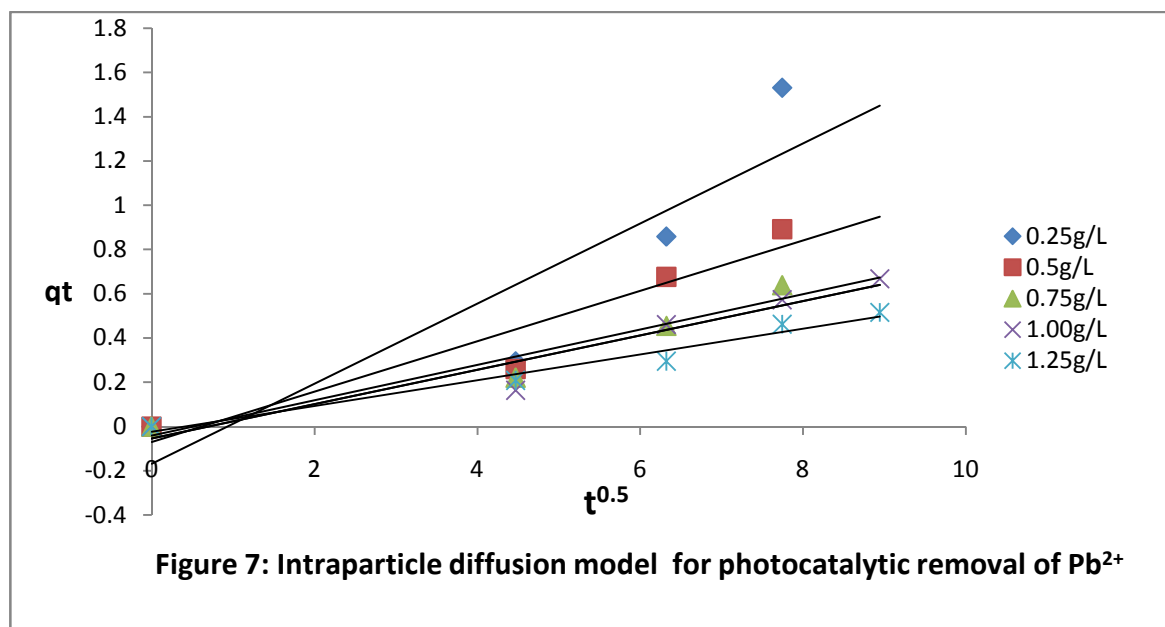


Figure 7: Intraparticle diffusion model for photocatalytic removal of  $Pb^{2+}$

Table 1: kinetic parameters for photocatalytic removal of  $Pb^{2+}$  in paint effluent

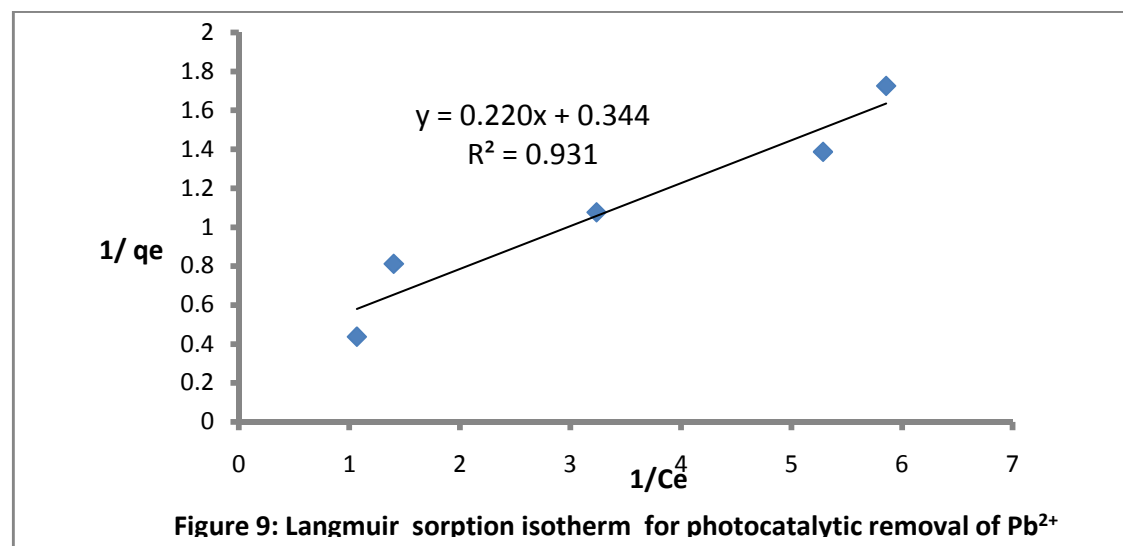
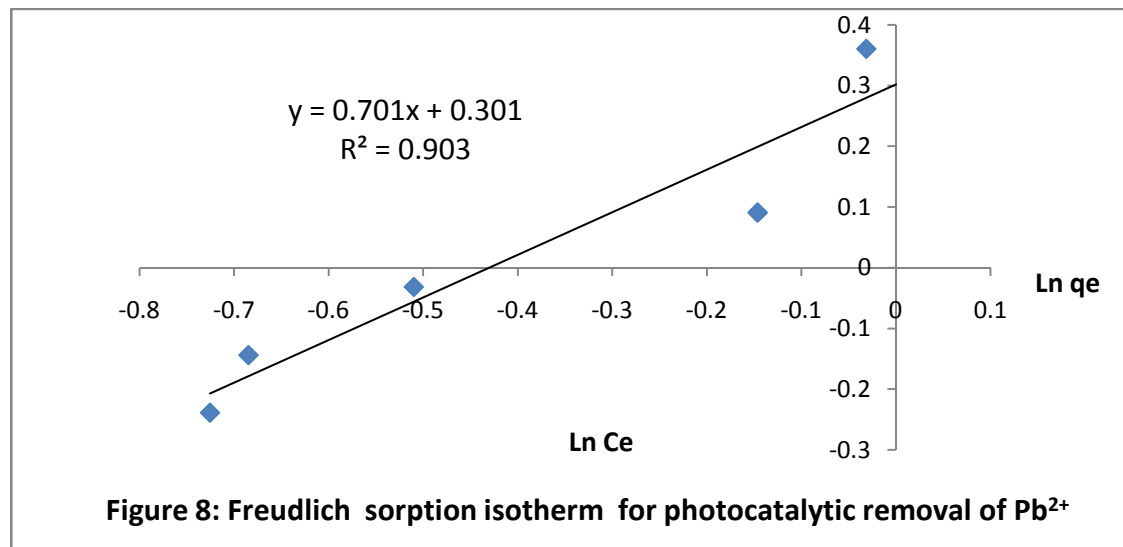
Catalyst dosage (g/L)	Pseudo-first order		Pseudo-second order		Intra-particle diffusion		
	$K_1$ ( $min^{-1}$ )	$R^2$	$K_2$ (g/mg.min)	$R^2$	$K_{int}$ (g/mg.min <sup>0.5</sup> )	$C_{id}$ (mg/g)	$R^2$
0.25	0.0179	0.9295	2.99E-3	0.8108	0.1810	-0.1683	0.8165
0.50	0.0164	0.9695	5.98E-3	0.8510	0.1138	-0.0704	0.9091
0.75	0.0120	0.9653	7.48E-3	0.9248	0.0799	-0.0415	0.9374
1.00	0.0194	0.9539	1.4E-2	0.8157	0.0777	-0.0545	0.9318
1.25	0.0177	0.9599	2.2E-2	0.9597	0.0582	-0.0236	0.9389

### 3.6 Adsorption Isotherms

Following the mechanism of heterogeneous photocatalysis, the substrate is pre-adsorbed on the surface of the catalyst prior to the UV illumination [36]. The data obtained from this study were fitted to Freundlich, Langmuir and Temkin isotherm models; and the linear plots are shown in Figures 8, 9 and 10, respectively. The isotherm parameters and correlation coefficients are presented in Table 2. Langmuir isotherm with a regression value,  $R^2$  of 0.931 and sorption capacity of 1.56L/mg gave the best description for the adsorption of  $Pb^{2+}$  on  $TiO_2$ . Langmuir isotherm was also reported in literature to have well described the photocatalytic decolourisation of acid orange 7 in aqueous solution [37]. The  $R_L$  value of 0.5814 was obtained in this study; thus the values of  $R_L$  between 0 and 1 indicate favourable adsorption [30]. Though the value of  $R^2$



(0.903) obtained from the Freundlich model was lower than the  $R^2$  value in Langmuir,  $1/n$  (adsorption strength) was 0.7015 which indicates favourability of the adsorption process [24]. The parameters  $K_T$  and  $b_T$  of the Temkin model were obtained at 305K;  $b_T$  referred to as the heat of sorption gave a positive value of 3.2015 KJ/mol indicating that the adsorption process was exothermic. This is in conformity with literature [38].



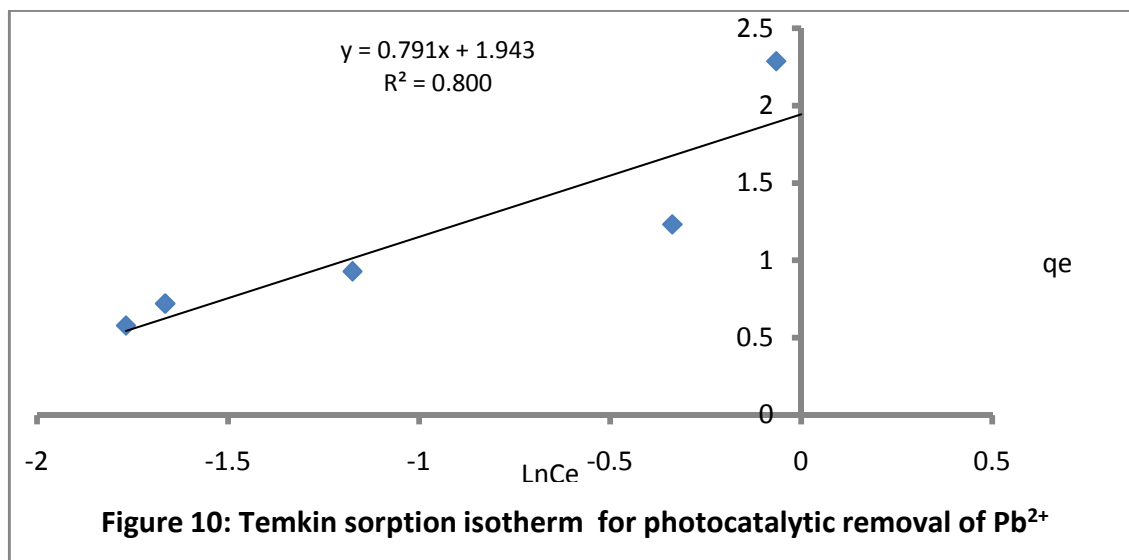


Figure 10: Temkin sorption isotherm for photocatalytic removal of  $Pb^{2+}$

Table 2: Adsorption isotherm parameters for photocatalytic removal of  $Pb^{2+}$  in paint effluent

Langmuir		Freundlich				Temkin			
$K_L$ (L/mg)	$R^2$	$R_L$	$K_f$ (mg/g)	$R^2$	$1/n$	$n$	$K_T$ L/mg	$b_T$ (kJ/mol)	$R^2$
1.56	0.931	0.1445	1.35	0.903	0.7015	1.43	11.65	3.2015	0.8003

#### 4.0 Conclusion

This study has shown that effluent from local paint manufacturing industry contains  $Pb^{2+}$  concentration of 3.796 mg/L which is well above the recommended acceptable discharge limit of  $< 1.0$  mg/L set by FEPA. The sunlight facilitated photocatalytic process for the removal of  $Pb^{2+}$  from aqueous solution was subjected to kinetic and sorption models. The pseudo-first order model gave the best description of the kinetic mechanism while the equilibrium data was best fitted to Langmuir isotherm. The rate constant and adsorption capacity based on pseudo-first order and Langmuir models were  $0.0194 \text{ min}^{-1}$  and  $1.56 \text{ L/mg}$ , respectively. The adsorption process is exothermic as the heat of sorption (3.2015) obtained from Temkin isotherm was greater than zero. It was shown in this work that sunlight facilitated photocatalytic process had an optimum  $TiO_2$  dosage of  $1 \text{ g/L}$  for effective removal of  $Pb^{2+}$  from aqueous solution as against  $0.9 \text{ g/L}$  with artificial UV-lamp induced photocatalysis reported in literature.

#### 5.0 References

- [1] Nielsen, M. H. and Rank, J. (1994). Screening of toxicity and genotoxicity in wastewater by the use of the *Allium* test. *Hereditas*, **121**: 249-254.
- [2] Bhaluro, B. B. and Adeko, A. B. (1981). Pollution survey of some textile mills in Lagos State. In: Proceedings of Federal Ministry of Water Resources (FMWR) Second National Conference on Water Pollution, 46 - 59.
- [3] Samuel, O. B., Osuala, F. and Odeigah, P. G. C., (2010). Cytogenotoxicity evaluation of two industrial effluents using *Allium cepa* assay. *African Journal of Environmental Science and Technology*, **4**(1): 21-27.
- [4] Oladele, E.O., Odeigah, P.G.C. and Yahaya, T. (2013). Hematotoxicity of paint effluent on Swiss albino mice. *The Pacific Journal of Science and Technology*, **14**(2): 397-398.
- [5] Abu, N.E. and Ezeugwu, S. C. (2008). Risk evaluation of industrial wastewater on plants using Onion (*Allium cepa* L.) Chromosome aberration assay. *Journal of Tropical Agriculture, Food, Environment and Extension*, **7**(3): 242-248.
- [6] Popoola, O. E., Bamgbose, O., Okonkwo, O. J., Arowolo, T. A., Popoola, A. O. and Awofolu, O. R. (2012). Heavy metals content in classroom dust of some public primary schools in metropolitan Lagos, Nigeria. *Research Journal of Environmental and Earth Sciences*, **4**(4): 460-465.
- [7] Olorunfemi, D. I., Ogieseri, U. M. and Akinboro, A., (2011). Genotoxicity screening of industrial effluents using Onion bulbs (*Allium cepa* L.). *Journal of Applied Science and Environmental Management*, **15**(1): 211 - 216.

- [8] Amenaghawon, N. A., Osarumwense, J. O., Aisien, F. A. and Olaniyan, O. K. (2014). Preparation and investigation of the photocatalytic properties of periwinkle shell ash for tartrazine decolourisation. *Journal of Mechanical Engineering and Sciences*, 7:1070-1084.
- [9] Ray, A. K. (1999). Design, Modeling and experimentation of a new large-scale photocatalytic reactor for Water Treatment. *Chemical Engineering Science*, 54:3113-3125.
- [10] Linsebigler, A. L., Lu, G. and Yates, J. T., Jr. (1995). Photocatalysis on TiO<sub>2</sub> Surfaces: Principles, mechanisms, and selected results. *Chemical Reviews*, 95: 735-758.
- [11] Priya, S.S., Premalatha, M and Anantharaman, N. (2008). Solar Photocatalytic Treatment of phenolic wastewater – Potential, Challenges and Opportunities. *Journal of Engineering and Applied Sciences*, 3(6):36-41.
- [12] Kavita K., Rubina, C. and Rameshwar, L. S. (2004). Treatment of hazardous organic and inorganic compounds through aqueous-phase photocatalysis: A Review. *Industrial and Engineering Chemistry Research*, 43:7683-7696.
- [13] Shaban, Y. A. (2013). Effective photocatalytic reduction of Cr(VI) by carbon modified (CM)-n-TiO<sub>2</sub> nanoparticles under solar irradiation. *World Journal of Nano Science and Engineering*, 3:154-160.
- [14] Rahimi, S., Ahmadian, M., Barati, R., Yousefi, N., Moussavi, S. P., Rahimi, K., Reshadat, S., Ghaseni, S., Gilani, N. R. and Fatehizadeh, A. (2014). Photocatalytic removal of cadmium (II) and lead (II) from simulated wastewater at continuous and batch system. *International Journal of Environmental Health Engineering*, 3(2):90-94.
- [15] Crittenden, J.C., Zhang, Y., Hand, D.W., Perram, D. L. and Marchand, E.G. (1996). Solar detoxification of fuel-contaminated groundwater using fixed bed photocatalysts” *Water Environment Research*, 68:3, 270-278.
- [16] Adeyi, O., Sunday, O., Ayanda, G. O. and Ganiyu, O. (2013). Adsorption kinetics and intraparticulate diffusivity of aniline blue dye onto activated plantain peels carbon. *Chemical Science Transactions*, 2(1): 294-300.
- [17] Martins, R. J. E., Vilar, V. J. P. and Boaventura, R. A. R. (2014). Kinetic modelling of cadmium and lead removal by aquatic Mosses. *Brazilian Journal of Chemical Engineering*, 31(1): 229-242.
- [18] Gerente, C., Lee V. K. C., Le Cloirec, P. and McKay, G. (2007). Application of chitosan for the removal of metals from wastewaters by adsorption – mechanisms and models review. *Critical Reviews in Environmental Science & Technology*, 37: 41–127.
- [19] Crank, J. (1970). *Mathematics of Diffusion*. Clarendon Press, Oxford, p.416.
- [20] Ho, Y. S. and McKay, G. (1999). The sorption of Lead (II) ions on Peat. *Water Research*, 33(2): 578–584.
- [21] Perju, M. M. and Dragan, E. S. (2010). Removal of azo dyes from aqueous solution using chitosan based composite hydrogels. *Ion Exchange Letters*, 3: 7 – 11.
- [22] Itodo, A. U., Abdulrahman, F. W., Hassan, L. G., Maigandi, S. A. and Itodo, H. U. (2010). Intra-particle diffusion and intra-particulate diffusivities of herbicide on derived activated carbon. *Researcher*, 2(2):74-86.
- [23] Hutson, N. D. and Yang, R. T. (2000). Adsorption. *Journal of Colloid Interface Science*, 3:189-195.
- [24] Foo, K. Y. and Hameed, B. H. (2010). Insight into the models of adsorption isotherm systems. *Chemical Engineering Journal*, 156:2-10.
- [25] Voudrias, E., Fytianos, F. and Bozani, E. (2002). Sorption description isotherms of dyes from aqueous solutions and Wastewater with different sorbent materials, *Global Nest, The International Journal*, 4(1): 75-83.
- [26] Mohan, S. and Karthikeyan, J. (1997). Removal of lignin and tannin color from aqueous solution by adsorption on to activated carbon solution. *Environmental Pollution*, 97: 183-187.
- [27] Vermeulan, T. H., Vermeulan, K. R. and Hall, L. C. (1966). Fundamental. *Industrial and Engineering Chemistry*, 5: 212-223.
- [28] Dada, A. O., Olalekan, A. P., Olatunya, A. M. and Dada, O. (2012). Langmuir, Freundlich, Temkin and Dubinin Radushkevich isotherms studies of equilibrium sorption of Zn<sup>2+</sup> unto phosphoric acid modified rice husk. *Journal of Applied Chemistry*, 3(1): 38-45.
- [29] Webber, T. N. and Chakravarti, R. K. (1974). Pore and solid diffusion models for fixed bed adsorbers. *Journal of America Institute of Chemical Engineering*, 20:228-238.
- [30] Elmorsi, T. M. (2011). Equilibrium isotherms and kinetic studies of removal of methylene blue dye by adsorption onto Miswak leaves as a natural adsorbent. *Journal of Environmental protection*, 2:817-827.
- [31] FEPA (1991). National Guidelines and Standards for Industrial Effluents, Gaseous Emissions and Hazardous Waste Management in Nigeria.
- [32] Inamdar, J. and Singh, S. K. (2008). Photocatalytic detoxification method for zero effluent discharge in dairy industry: Effect of operational parameters. *International Journal of Chemical and Biological Engineering*, 1(4): 160-164.
- [33] Daneshvar, N., Aber, S., Seyed Dorraji, N.S., Khataee, A. R. and Rasoulifard, M. H. (2007). Preparation and investigation of photocatalytic properties of ZnO nanocrystals: Effect of operational parameters and kinetic study, *World Academy of Science, Engineering and Technology*, 29:267-272.

- [34] Randhawa, N. S., Das, N. N and Jana, R. K. (2013). Adsorptive remediation of Cu(II) and Cd(II) contaminated water using manganese nodule leaching residue, *Desalination and water treatment*, 22-24(52):4197-4211.
- [35] Biyan, J., Fei, S., Hu, G., Zheng, S., Zhang, Q. and Xu, Z. (2009). Adsorption of methyl tert-butyl ether (MTBE) from aqueous solution by porous polymeric adsorbent. *Journal of Hazard material*, 161(1):81-87.
- [36] Lin, H. and Valsaraj, K. T. (2005). Development of an optical fiber monolith reactor for photocatalytic wastewater treatment. *Journal of Applied Electrochemistry*, **35** (7): 699-708.
- [37] Aisien, F.A., Amenaghawon, N.A., Osarumwense, J.O. and Ochei, D.K. (2014). Periwinkle shell ash facilitated photocatalytic decolourisation of acid Orange 7 in aqueous solution. *44th annual conference of the Nigerian Society of Chemical Engineers Conference proceedings*, Owerri, Nigeria, 315-326.
- [38] Negulescu, A., Patrulea, V., Mincea M. and Moraru, C. (2014). The adsorption of tartrazine, congo red and methyl orange on chitosan beads. *Digest Journal of Nanomaterials and Biostructures*, 9:45-52.